WILEY | Hindawi

Research Article

SNHG12 Promotes Autophagy by Blocking the mTOR-Primary Cilia-mTOR Loop via Activating the miR-181a-5p/miR-138-5p-INPP5E Axis in Chondrocyte

Weijia Feng,[1] Lei Liu,[2] Lin Sha,[1] Zhenkai Wu ⓘ,[1] and Jing Ding ⓘ[1]

[1]*Department of Pediatric Orthopaedics, Xinhua Hospital, School of Medicine, Shanghai Jiao Tong University, Shanghai 200092, China*
[2]*Department of Orthopaedics, The Affiliated Yixing Hospital of Jiangsu University, Yixing 214200, Jiangsu, China*

Correspondence should be addressed to Zhenkai Wu; wuzhenkai@xinhuamed.com.cn and Jing Ding; dingjing@xinhuamed.com.cn

Diseases related to cartilage abnormalities pose a serious threat to human health. Normal cartilage contains only one type of cell, chondrocytes. This study aims to investigate the impact of inositol polyphosphate-5-phosphatase E (INPP5E) on chondrocytes and its underlying mechanisms. Following transfection of small interfering RNA INPP5E into chondrocytes, real-time quantitative PCR (RT-PCR) and western blot (WB) assays were conducted to detect the expression of intraflagellar transport 88 (IFT88), Bcl-2-interacting protein 1 (Beclin1), microtubule-associated protein 1 light chain 3 alpha (MAP1LC3A), microtubule-associated protein 1 light chain 3 beta (MAP1LC3B), phosphoinositide 3-kinase (PI3K), protein kinase B (Akt), mammalian target of rapamycin (mTOR), collagen type II alpha 1 chain (COL2A1), and cyclin D1 (CCND1). Furthermore, immunofluorescence was used to detect the expression of acetylated α-tubulin and microtubule-associated protein 1 light chain 3 (LC3) II. RT-PCR, WB, and the dual luciferase assay demonstrated the regulation between SNHG12, hsa-miR-181a-5p, hsa-miR-138-5p, and INPP5E. Functional recovery experiments were used to observe the regulation of these factors on IFT88, Beclin1, LC3 I, LC3 II, p-PI3K, p-Akt, p-mTOR, collagen II, and cyclin D1 in chondrocytes. The results showed that silencing INPP5E inhibited the mRNA and protein expressions of the investigated factors in chondrocytes. SNHG12 promoted INPP5E expression by inhibiting hsa-miR-181a-5p or hsa-miR-138-5p, which resulted in regulation of the expression of various factors via the hsa-miR-181a-5p/hsa-miR-138-5p-INPP5E axis in chondrocytes. These findings provide a theoretical basis for the treatment of patients with cartilage-related abnormalities.

1. Introduction

It has been reported that there are numerous diseases associated with cartilage abnormalities, including chondrocalcinosis, arthropathies, and relapsing polychondritis, which can severely impact human health [1]. Chondrocytes are the only cell type found in normal cartilage, and a thorough understanding of their pathology and function is crucial for both cartilage repair and engineering [2]. Primary cilia are multifunctional sensory organelles that regulate various signal transduction pathways and cellular activities, playing a critical role in the regulation of chondrogenesis [3].

Inositol polyphosphate-5-phosphatase E (INPP5E) is a transporter protein located on the primary cilia membrane, and it plays an important role in regulating the development and homeostasis of primary cilia [4]. INPP5E is also responsible for maintaining the stability of primary cilia [5]. However, mutations or absences of INPP5E can lead to primary ciliary signal transduction deficiencies [4]. Primary cilia, acting as mechanical sensors, are instrumental in limiting rapamycin complex 1 (mTORC1) signal transduction by converting mechanical signals into chemical activity [6]. As a result, INPP5E may be involved in mTORC1 signal transduction by regulating primary cilia.

Moreover, a potential link between primary cilia and autophagy has recently been proposed, which could increase our understanding of the pathogenesis of cartilage-related diseases [7]. Autophagy is an intracellular degradation system that plays a role in maintaining intracellular energy metabolism homeostasis and has been shown to modulate the function of damaged chondrocytes [8]. In addition, each step of autophagy is regulated by the target protein mTORC1 [9]. Therefore, INPP5E may be involved in regulating autophagy via primary cilia-mTORC1 signal transduction.

The competitive endogenous RNA (ceRNA) hypothesis proposes that transcripts which exhibit shared microRNA (miRNA) binding sites compete for posttranscriptional control [10]. However, research on the mechanism of ceRNA involving INPP5E is limited. miR-181a-5p and miR-138-5p are microRNAs that have been implicated in autophagy [11–14]. They are known to regulate gene expression by binding to the 3′ untranslated region (UTR) of their target mRNAs. One of the targets of miR-181a-5p and miR-138-5p is INPP5E. Studies have shown that SNHG12 acts as a competing endogenous RNA (ceRNA) for miR-181a-5p and miR-138-5p [15, 16]. As a result, we speculate that SNHG12 may compete with INPP5E mRNA for binding to these microRNAs, thereby sequestering them and preventing their binding to INPP5E 3′ UTR. This ceRNA activity of SNHG12 may lead to increased expression of INPP5E, resulting in altered mTOR signaling and potential downstream effects on autophagy, which may reveal the relationship between SNHG12 and the miR-181a-5p/miR-138-5p-INPP5E axis, suggesting a regulatory network in which SNHG12 acts as a ceRNA to modulate the expression of INPP5E by competing with miR-181a-5p and miR-138-5p. The purpose of this study was to explore the crucial connections between ceRNA, INPP5E, primary cilia, autophagy, mTORC1, and chondrocytes and to provide new insights into the physiological mechanisms associated with chondrocytes.

2. Materials and Methods

2.1. Bioinformatics Information. The next generation sequencing of 23 cartilage knee samples was conducted using the Affymetrix Human Gene 1.1 ST Array (transcript version) platform (HuGene-1_1-st). The R language software package "limma" was utilized to identify differentially expressed genes (DEGs) between the INPP5E-low expression ($N = 11$) and INPP5E-high expression ($N = 12$) groups. A significance threshold of $P < 0.05$ and fold change ≥2 were applied. The Kyoto Encyclopedia of Genes and Genomes (KEGG) database (https://www.kegg.jp/kegg/rest/keggapi.html) was employed to obtain the latest KEGG pathway gene annotation as the background for mapping the genes. Enrichment analysis was performed using the R software package "clusterProfiler" (version 3.14.3), and $P < 0.05$ was considered as a significant difference. For gene set enrichment analysis (GSEA), we obtained the GSEA software (version 3.0) from the GSEA Database (https://software.broadinstitute.org/gsea/index.jsp). We downloaded c2.cp.kegg.v7.4.symbols.gmt from the Molecular Signatures Database (https://www.gsea-msigdb.org/gsea/downloads.jsp) to evaluate the pathways and molecular mechanisms. A significance threshold of $P < 0.05$ was applied.

2.2. Cell Culture. The C28/I2 cell line, composed of normal human chondrocytes, was provided by Zhongqiao Xinzhou Biotechnology Co., LTD (Shanghai, China). The cells were cultured in the RPMI-1640 medium, supplemented with 10% FBS and 100 U/mL penicillin and streptomycin, all provided by Zhongqiao Xinzhou Biotechnology Co., LTD, Shanghai, China. The cells were maintained in a 5% CO_2 humidified incubator at 37°C.

2.3. Cell Transfection and Treatment. $1 * 10^6$ C28/I2 cells were inoculated into 6-well plates and transfected with the corresponding plasmid or small interfering RNA (siRNA) using lip3000. The details of the plasmids and siRNAs used are presented in Supplement Table 1. Follow-up experiments were conducted 72 hours after transfection. All reagents were provided by Guangdong Ruibo Biotechnology Co., LTD., China.

2.4. Chloral Hydrate (CH) and Rapamycin (Rapa) Treatment. CH plays a well-established role in chemically removing primary cilia [17]. To remove primary cilia from C28/I2 cells, the cells ($2 * 105$ cells/well) were cultured in the RPMI-1640 medium containing 8 mM CH (Sigma-Aldrich, Merck, USA) for 48 hours. Rapamycin (HY-10219, Med-ChemExpress, China) is a potent and specific inhibitor of mTOR. For the Rapa group, C28/I2 cells ($2 * 105$ cells/well) were cultured in the RPMI-1640 medium containing 0.1 nM Rapa for 48 hours. To test the combined effect of CH and Rapa, C28/I2 cells ($2 * 105$ cells/well) were cultured in the RPMI-1640 medium containing 8 mM CH and 0.1 nM RAPA for 48 hours.

2.5. Real-Time Fluorescence Quantitative PCR (RT-PCR). Total RNA was extracted from the cells using Trizol. The total RNA was reverse-transcribed into cDNA using RT Master Mix for qPCR (gDNA digester plus, MedChemExpress, China). PCR detection was performed using POWER SYBR GREEN PCR MASTER (4368708, Applied Biosystems, USA). The primer sequences used in this study are provided in Supplementary Table 2. The relative expression levels were calculated using the $2^{-\triangle\triangle Ct}$ method.

2.6. Western Blotting (WB). The proteins present in C28/I2 cells were extracted using the radioimmunoprecipitation assay buffer (RIPA) and quantified through the bicinchoninic acid (BCA) kit (C503021, Sangong Bioengineering Co., LTD., Shanghai, China). The proteins were then added to sodium dodecyl sulfate-polyacrylamide gel electrophoresis (SDS-PAGE) and transported to polyvinylidene difluoride membranes (Millipore, USA). The transferred membranes were blocked with Tris-buffered saline with Tween 20

(TBS-T) (0.1% Tween 20 and TBS) containing 5% skim milk for 30 minutes and were subsequently incubated overnight at 4°C with primary antibodies (refer to Supplement Table 3). Following this, the membranes were washed three times for 10 minutes with TBS-T and incubated for an hour at 25°C with HRP-conjugated secondary antibodies (refer to Supplement Table 3).Visualization of the protein bands was achieved by the application of enhanced chemiluminescence using an enhanced chemiluminescence (ECL) kit (AB133406, Abcam, USA). Images were obtained with SigmaTel software V2.0, and protein density was computed through the use of Image Lab software V3.0.

2.7. Immunofluorescence. The cells were fixed using 4% paraformaldehyde in phosphate-buffered saline (PBS) for 15 minutes at 25°C. Next, the cells were permeabilized with 50 lg/mL digitonin in PBS containing 0.1% gelatin for 5 minutes at RT, followed by blocking with PBS containing 0.1% gelatin for 30 minutes at RT. The cells were then incubated with primary antibodies in PBS containing 0.1% gelatin for 60 minutes and subsequently washed thrice with PBS. The appropriate secondary antibodies were then added, and the cells were incubated in PBS containing 0.1% gelatin for 50 minutes. The coverslips were mounted onto slides using a PermaFluor mountant medium (Thermo Fisher Scientific, USA), and the samples were observed under a FluoView 1000-D confocal microscope equipped with a 63x/NA 1.40 oil immersion objective lens (Olympus, Japan) or a Delta Vision microscopic system equipped with a 60x/NA 1.42 oil immersion objective lens (Applied Precision). The images were deconvolved using Delta Vision SoftWoRx software. Immunofluorescent double staining was performed using the anti-LC3B antibody (EPR18709), autophagosome marker (ab192890, Abcam, USA), anti-alpha Tubulin (acetyl K40) (EPR16772) (ab218591, Abcam, USA), and Alexa Fluor 594 labeled goat anti-rabbit IgG (H + L; 33112ES60, Yeasen, Shanghai).

2.8. Luciferase Report. The miRNA targets of INPP5E were predicted using the TargetScan database (https://www.targetscan.org/vert_80/). Meanwhile, the targets of hsa-miR-181a-5p and hsa-miR-138-5p on long noncoding RNA (lncRNA) were predicted via the starBase database (https://starbase.sysu.edu.cn/). A total of $1 * 105$ C28/I2 cells were inoculated into 96-well plates, followed by transfection of a luciferase reporter plasmid consisting of Firefly (Luciferase Reporter Assay Substrate Kit, Firefly, AB228530, ABCAM, USA) and Renilla (Luciferase Reporter Assay Substrate Kit, Renilla, AB228546, USA) after 24 hours. The pMIR-INPP5E-mutant (mut) $3'$ UTR plasmid, pMIR-SNHG12-mut-1 $3'$ UTR plasmid, and pMIR-SNHG12-mut-2 $3'$ UTR plasmid, constructed based on the binding sites predicted by the TargetScan database and the starBase database, represented the mutated plasmids. Heyuan Biology Co., LTD. (Shanghai, China) provided pMIR- INPP5E-wild type (WT) $3'$ UTR plasmid and all mutated plasmids. The cotransfection of each plasmid with a luciferase reporter plasmid was conducted for 48 hours. Afterward, $100\,\mu l$ Stop&Glo

reagent was added per well, and fluorescence was detected at a wavelength of 480 nm (SpectraMax M2e Molecular Devices, USA).

2.9. Statistical Analysis. SPSS 21.0 (International Business Machines Corporation, NY, USA) was used for data collection, expressed as mean ± standard deviation (SD). All experiments were performed independently at least three times; the comparison method of the two groups was Wilcoxon tests. $P < 0.05$ was considered statistically significant.
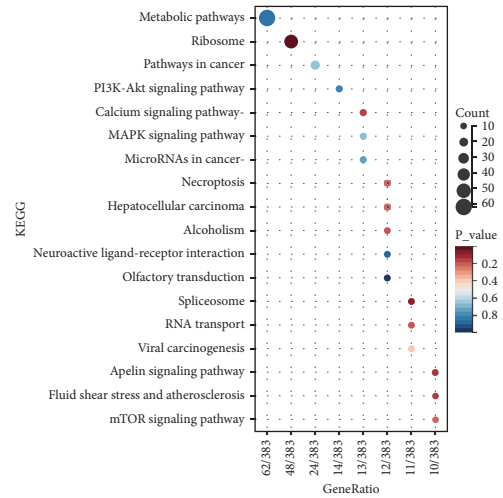
3. Results

3.1. INPP5E Deactivated the PI3K-Akt-mTOR Signaling Pathway In Vitro. Based on the GSE43191 dataset, we have divided the samples into two groups—the INPP5E-low expression group ($N = 11$) and the INPP5E-high expression group ($N = 12$). By using $P < 0.05$ and fold change ≥2 as the screening criteria, we found 998 genes that were differentially expressed in the INPP5E-high expression group compared to the INPP5E-low expression group (Figure 1(a)). KEGG analysis (Figure 1(b)) and GSEA analysis (Figure 1(c)) further showed that these genes were significantly enriched in the PI3K-Akt and mTOR signaling pathways. Hence, it is possible that INPP5E plays a vital role in regulating the PI3K-Akt and mTOR signaling pathways. To validate this hypothesis, we conducted an RT-PCR detection and found that the mRNA expression of INPP5E was significantly reduced in the si-INPP5E-2 and si-INPP5E-3 groups compared to the control or negative control (NC) group (Figure 1(d)). In addition, we used WB detection and observed a significant reduction in the protein expression of INPP5E in the si-INPP5E-2 group compared to the WT or NC group (Figure 1(e)). Furthermore, silencing INPP5E resulted in upregulation of the mRNA expression of PI3K, Akt, and mTOR in chondrocytes (Figure 1(f)). Though we did not observe a significant difference in the protein expression of PI3K, Akt, and mTOR between the control, NC, and si-INPP5E-2 groups, silencing INPP5E led to upregulation of the protein expression of p-PI3K, p-Akt, and p-mTOR in chondrocytes (Figure 1(g)). Hence, it can be concluded that silencing INPP5E promoted the activation of the PI3K-Akt-mTOR signaling pathway in vitro.

3.2. INPP5E Promotes Autophagy via Regulating the mTOR-Primary Cilia-mTOR Loop. Inhibition of INPP5E expression resulted in decreased mRNA and protein levels of IFT88, Beclin1, and LC3 I/II, indicating a reduction in primary cilia and autophagy (Figures 2(a) and 2(b)). Moreover, treatment with CH downregulated the expression of IFT88, Beclin1, MAP1LC3A/B, PI3K, Akt, and mTOR at the mRNA level (Figure 2(c)) and the protein level for IFT88, Beclin1, LC3 I/II, and phosphorylated forms of PI3K, Akt, and mTOR (Figure 2(d)). These findings imply that the inhibition of primary cilia leads to decreased autophagy and inhibits the activation of the PI3K-Akt-mTOR signaling pathway in chondrocytes. In addition, the effects of INPP5E and mTOR on the protein expression of ace-tubulin and
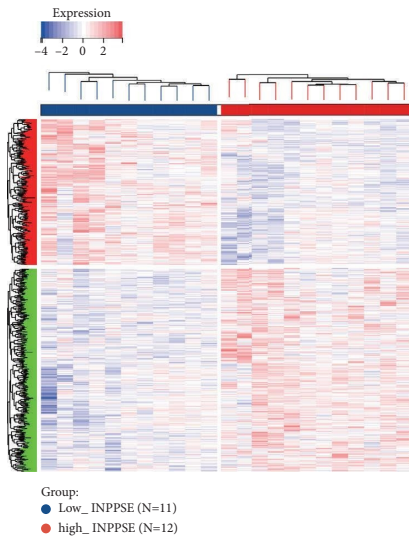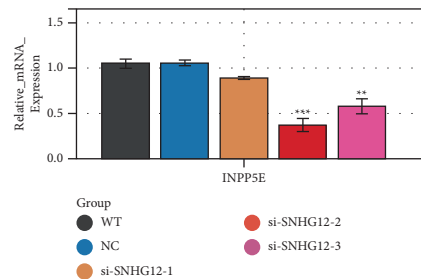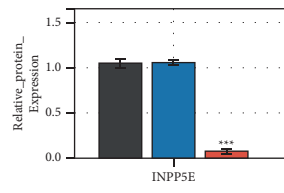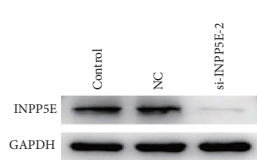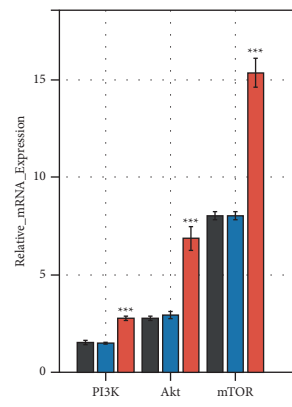
(a)

(b)
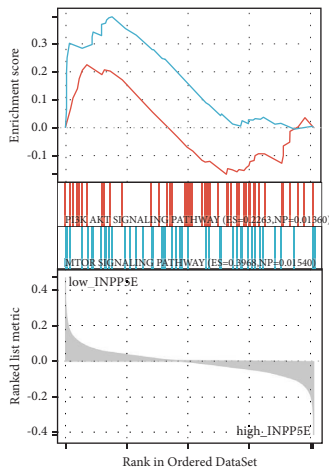
(c)

(d)
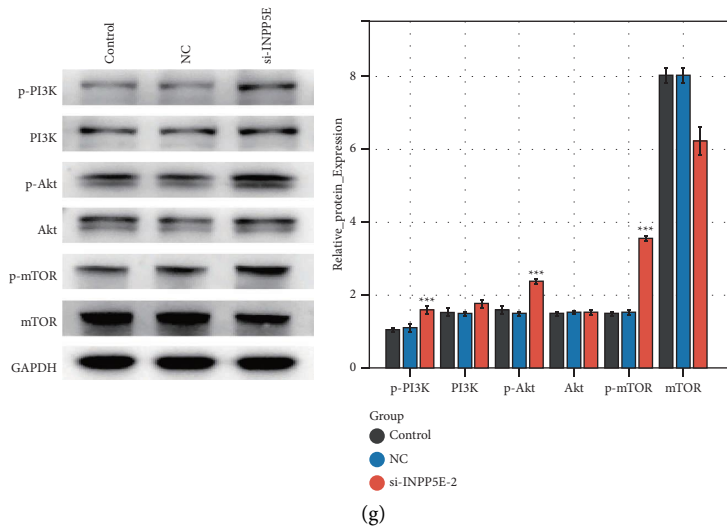

(e)

(f)

Figure 1: Continued.

(g)

Figure 1: Silencing INPP5E activates the PI3K-Akt-mTOR signaling pathway in vitro. (a) We divided the samples into the INPP5E-low expression ($N = 11$) group and the INPP5E-high expression ($N = 12$) group in the GSE43191 dataset. Using $P < 0.05$ and fold change ≥ 2 as screening criteria, a hub of 998 DEGs were identified. (b) KEGG analysis and (c) GSEA analysis were used to analysis the pathway mechanism involved in these 998 DEGs. (d) RT-PCR assay was used to detect the expression of INPP5E. (e) WB assay was used to detect the expression of INPP5E. (f) RT-PCR assay was used to detect the expression of PI3K, Akt, and mTOR. (g) WB assay was used to detect the expression of PI3K, p-PI3K, Akt, p-Akt, mTOR, and p-mTOR. Notes: $^*p < 0.05$, $^{**}p < 0.01$, and $^{***}p < 0.001$ compared with the control.

LC3 I/II were investigated. INPP5E knockdown decreased the levels of ace-tubulin and LC3 I/II, while mTOR activation induced their expression, which was reversed by INPP5E silencing (Figure 2(e)). Furthermore, in the CH-treated group, there was also a reduction in ace-tubulin and LC3 I/II expression, which was rescued by rapamycin treatment (Figure 2(e)). These results suggest that the regulation of autophagy by INPP5E occurs through the modulation of primary cilia-induced mTOR inactivation. In summary, the present study provides evidence that INPP5E inhibition reduces autophagy by promoting PI3K-Akt-m-TOR signaling activation, whereas activated PI3K-Akt-m-TOR signaling further downregulates autophagy by inhibiting primary cilia. These findings shed new light on the mechanisms underlying the regulation of autophagy and primary cilia in chondrocytes.

3.3. The SNHG12-hsa-miR-181a-5p/hsa-miR-138-5p-INPP5E ceRNA Network In Vitro. The TargetScan database was used to predict miRNAs that might bind to INPP5E (Supplement Figure 1). It was reported that overexpression of hsa-miR-4262 promoted autophagy in chondrocyte [18]. However, overexpression of hsa-miR-181a-5p inhibited hunger-induced cardiac autophagy [19], and overexpression of hsa-miR-138-5p inhibited MnCl2-induced autophagy in SH-SY5Y cells [14]. Therefore, we speculated that high expression of hsa-miR-181a-5p and hsa-miR-138-5p might inhibit autophagy of chondrocytes by inhibiting INPP5E. Compared with the control or NC group, the expression of hsa-miR-181a-5p was increased significantly in the mimic-1 group (Figure 3(a)). Overexpression of hsa-miR-181a-5p inhibited the mRNA (Figure 3(b)) and protein (Figure 3(c)) expression of INPP5E in chondrocytes. Compared with the

mimic-NC group, the relative intensity of fluorescence in the mimic-1 group was reduced significantly in INPP5E-WT chondrocytes. However, there was no significant difference of the relative intensity of fluorescence between the mimic-NC and mimic-1 groups in INPP5E-Mut chondrocytes via the dual luciferase reported assay (Figure 3(d)). Compared with the control or NC group, the expression of hsa-miR-138-5p was increased significantly in the mimic-2 group (Figure 3(e)). Overexpression of hsa-miR-138-5p inhibited the mRNA (Figure 3(f)) and protein (Figure 3(g)) expression of INPP5E in chondrocytes. Compared with the mimic-NC group, the relative intensity of fluorescence in the mimic-2 group was reduced significantly in INPP5E-WT chondrocytes. However, there was no significant difference of the relative intensity of fluorescence between the mimic-NC and mimic-2 groups in INPP5E-Mut chondrocytes via the dual luciferase reported assay (Figure 3(h)). Based on the starBase database, we found that 5 lncRNAs (RP11-170L3.8, AC006262.5, RP11-615I2.7, SNHG12, and RP11-478C19.2) may be common targets of hsa-miR-181a-5p and hsa-miR-138-5p (Figure 3(i)). The predicted binding sites between the mRNA of SNHG12 and hsa-miR-181a-5p and hsa-miR-138-5p are also shown in Figure 3(i). It showed that SNHG12 mRNA may have multiple binding sites with hsa-miR-181a-5p and hsa-miR-138-5p, indicating that hsa-miR-181a-5p and hsa-miR-138-5p may regulate the expression of SNHG12. Overexpression of SNHG12 is reported to promote autophagy of the SH-SY5Y cells [20]. Therefore, SNHG12 may promote chondrocyte autophagy through upregulation of INPP5E. Compared with the control or NC group, the expression of SNHG12 was reduced significantly in the si-SNHG12-2 and si-SNHG12-3 groups (Figure 3(j)). Silencing SNHG12 promoted the expression of hsa-miR-181a-5p and hsa-miR-138-5p in chondrocytes (Figure 3(k)).

Compared with the mimic-NC group, the relative intensity of fluorescence in the mimic-1 group was reduced significantly in SNHG12-WT chondrocytes. However, there was no significant difference of the relative intensity of fluorescence between the mimic-NC and mimic-1 groups in SNHG12-Mut-1 chondrocytes via the dual luciferase reported assay (Figure 3(l)). Compared with the mimic-NC group, the relative intensity of fluorescence in the mimic-2 group was reduced significantly in SNHG12-WT chondrocytes. However, there was no significant difference of the relative intensity of fluorescence between the mimic-NC and mimic-2 groups in SNHG12-Mut-2 chondrocytes via the dual luciferase reported assay (Figure 3(m)). Together, SNHG12 promoted the expression of INPP5E via decreasing hsa-miR-181a-5p and hsa-miR-138-5p expression in chondrocytes.

3.4. SNHG12 Inhibits Primary Cilia and Autophagy via the hsa-miR-181a-5p/hsa-miR-138-5p-INPP5E Axis in Chondrocytes.
Compared with the control or NC group, the mRNA (Figure 4(a)) and protein (Figure 4(b)) expression of INPP5E was enhanced significantly in the overexpression (OE)-INPP5E group. Compared with the control or NC group, the mRNA (Figure 4(c)) and protein (Figure 4(d)) expression of INPP5E was reduced significantly in the si-INPP5E group. Compared with the control or NC group, the mRNA (Figure 4(e)) and protein (Figure 4(f)) expression of IFT88, Beclin1, LC3 I, and LC3 II was reduced significantly in the mimic-1 group. Compared with the mimic-1 group, the mRNA (Figure 4(e)) and protein (Figure 4(f)) expression of IFT88, Beclin1, and LC3 I was enhanced significantly in the mimic-1 + OE-INPP5E group. Compared with the control or NC group, the mRNA (Figure 4(g)) and protein (Figure 4(h)) expression of IFT88, Beclin1, LC3 I, and LC3 II was reduced significantly in the mimic-2 group. Compared with the mimic-2 group, the mRNA (Figure 4(g)) and protein (Figure 4(h)) expression of IFT88, Beclin1, and LC3 I was enhanced significantly in the mimic-2 + OE-INPP5E group. Compared with the control or NC group, the mRNA (Figure 4(i)) and protein (Figure 4(j)) expression of IFT88, Beclin1, LC3 I, and LC3 II was reduced significantly in the si-SNHG12 group. Compared with the si-SNHG12 group, the mRNA (Figure 4(i)) and protein (Figure 4(j)) expression of IFT88, Beclin1, and LC3 I was enhanced significantly in the si-SNHG12 + OE-INPP5E group. Compared with the control or NC group, the protein expression of ace-tubulin and LC3 I/II was increased significantly in the OE-INPP5E group. Compared with the OE-INPP5E group, the protein expression of ace-tubulin and LC3 I/II was decreased significantly in the si-SNHG12 + OE-INPP5E group, mimic-1 + OE-INPP5E group, or mimic-2 + OE-INPP5E group (Figure 4(k)). Together, silencing SNHG12 promoted primary cilia and autophagy via the hsa-miR-181a-5p/hsa-miR-138-5p-INPP5E axis in chondrocytes.

3.5. SNHG12 Deactivates the PI3K-Akt-mTOR Signaling Pathway via the hsa-miR-181a-5p/hsa-miR-138-5p-INPP5E Axis In Vitro.
Compared with the control or NC group, the mRNA expression of PI3K, Akt, and mTOR was enhanced in the mimic-1 group. Compared with the mimic-1 group, the mRNA expression of PI3K, Akt, and mTOR was reduced in the mimic-1 + OE-INPP5E group (Figure 5(a)). Compared with the control or NC group, the protein expression of p-PI3K, p-Akt, and p-mTOR was enhanced in the mimic-1 group. Compared with the mimic-1 group, the protein expression of p-PI3K, p-Akt, and p-mTOR was reduced in the mimic-1 + OE-INPP5E group (Figure 5(b)). However, there was no significance of the protein expression of PI3K, Akt, and mTOR among the control, NC, mimic-1, and mimic-1 + OE-INPP5E groups in chondrocytes (Figure 5(b)). Compared with the control or NC group, the mRNA expression of PI3K, Akt, and mTOR was enhanced in the mimic-2 group. Compared with the mimic-1 group, the mRNA expression of PI3K, Akt, and mTOR was reduced in the mimic-2 + OE-INPP5E group (Figure 5(c)). Compared with the control or NC group, the protein expression of p-PI3K, p-Akt, and p-mTOR was enhanced in the mimic-1 group. Compared with the mimic-2 group, the protein expression of p-PI3K, p-Akt, and p-mTOR was reduced in the mimic-2 + OE-INPP5E group (Figure 6(d)). However, there was no significance of the protein expression of PI3K, Akt, and mTOR among control, NC, mimic-2, and mimic-2 + OE-INPP5E group in chondrocytes (Figure 5(d)). Compared with the control or NC group, the mRNA expression of PI3K, Akt, and mTOR was enhanced in the si-SNHG12 group. Compared with the si-SNHG12 group, the mRNA expression of PI3K, Akt, and mTOR was reduced in the si-SNHG12 + OE-INPP5E group (Figure 5(e)). Compared with the control or NC group, the protein expression of p-PI3K, p-Akt, and p-mTOR was enhanced in the si-SNHG12 group. Compared with the si-SNHG12 group, the protein expression of p-PI3K, p-Akt, and p-mTOR was reduced in the si-SNHG12 + OE-INPP5E group (Figure 6(f)). However, there was no significance of the protein expression of PI3K, Akt, and mTOR among control, NC, si-SNHG12, and si-SNHG12 + OE-INPP5E groups in chondrocytes (Figure 5(f)). Together, silencing SNHG12 activated the PI3K-Akt-mTOR signaling pathway via the hsa-miR-181a-5p/hsa-miR-138-5p-INPP5E axis in chondrocytes.

3.6. SNHG12 Promotes the Expression of Collagen II and Cyclin D1 via the hsa-miR-181a-5p/hsa-miR-138-5p-INPP5E Axis In Vitro.
Compared with the control or NC group, the mRNA expression of COL2A1 and CCND1 was reduced and the protein expression of collagen II and cyclin D1 was reduced in the si-INPP5E group (Figures 6(a) and 6(b)). Compared with the control or NC group, the mRNA expression of COL2A1 and CCND1 was reduced and the protein expression of collagen II and cyclin D1 was reduced in the mimic-1 group (Figures 6(c) and 6(d)) and mimic-2 group (Figures 6(e) and 6(f)). Compared with the mimic-1 group or the mimic-2 group, the mRNA expression of COL2A1 and CCND1 was increased and the protein expression of collagen II and cyclin D1 was increased in the mimic-1 + OE-INPP5E group (Figures 6(c) and 6(d)) and the mimic-2 + OE-INPP5E group (Figures 6(e) and 6(f)), respectively. Compared with the control or NC group, the mRNA expression of COL2A1 and CCND1 was reduced and
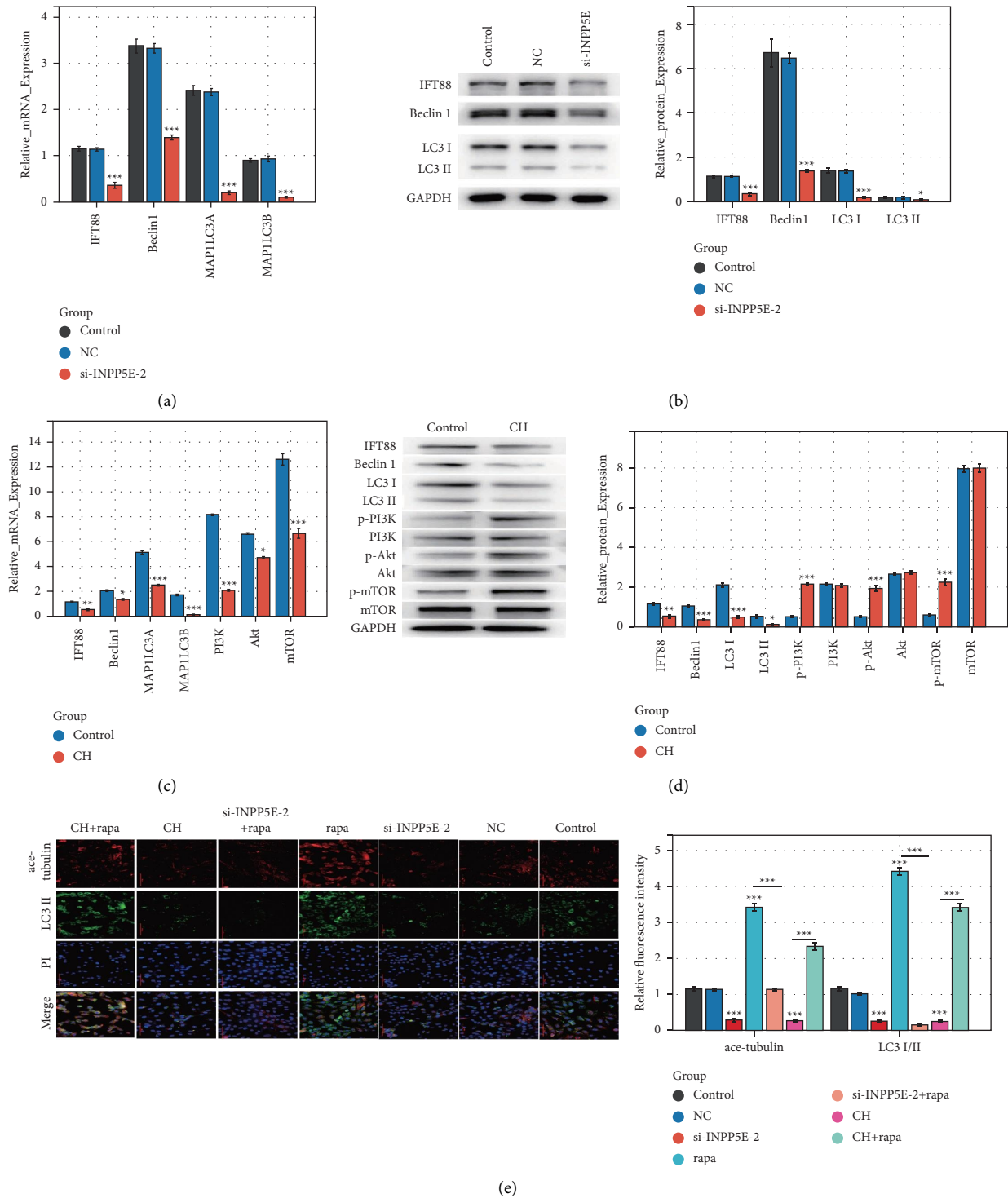
(a)

(b)

(c)

(d)

(e)

FIGURE 2: Silencing INPP5E inhibits autophagy via regulating the mTOR-primary cilia-mTOR loop in vitro. (a) RT-PCR assay was used to detect the mRNA expression of IFT88, Beclin1, MAP1LC3A, and MAP1LC3B in control, NC, and si-INPP5E-2 groups. (b) WB assay was used to detect the protein expression of IFT88, Beclin1, LC3 I, and LC3 II in control, NC, and si-INPP5E-2 groups. (c) RT-PCR assay was used to detect the mRNA expression of IFT88, Beclin1, MAP1LC3A, MAP1LC3B, PI3K, Akt, and mTOR in control and CH-treated groups. (d) WB assay was used to detect the protein expression of IFT88, Beclin1, LC3 I, LC3 II, p-PI3K, PI3K, p-Akt, Akt, p-mTOR, and mTOR in control and CH-treated groups. (e) Ace-tubulin was used to label primary cilia, and LC3 II was used to label autophagy via immuno-fluorescence assay. Notes: $^*p < 0.05$, $^{**}p < 0.01$, and $^{***}p < 0.001$ compared with the control or between the indicated groups.

(a)　　(b)　　(c)　　(d)

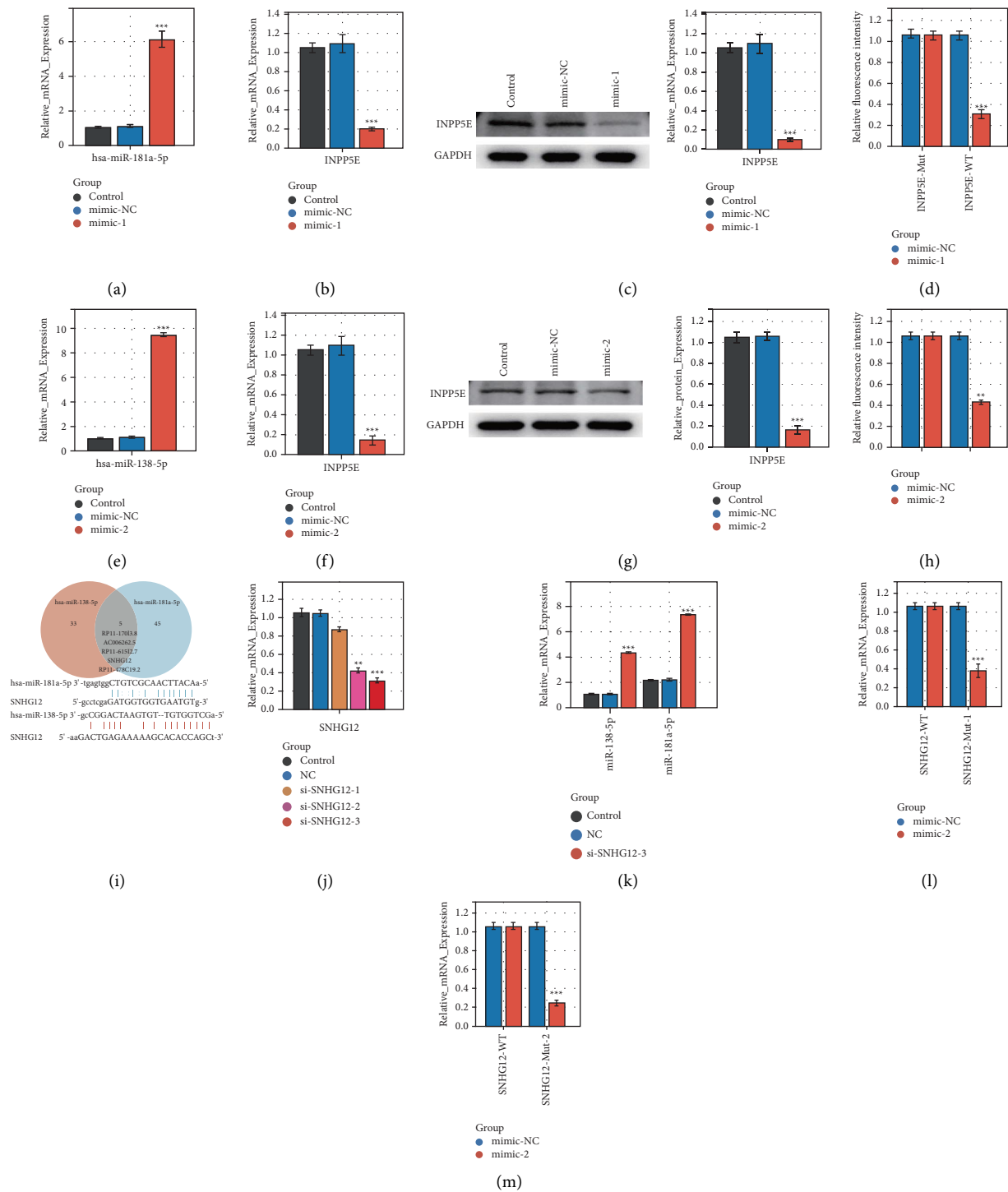(e)　　(f)　　(g)　　(h)

(i)　　(j)　　(k)　　(l)

(m)

Figure 3: SNHG12 promotes the expression of INPP5E via hsa-miR-181a-5p/hsa-miR-138-5p in vitro. (a) RT-PCR assay was used to detect the expression of hsa-miR-181a-5p in control, mimic-NC, and mimic-1 groups. (b) RT-PCR assay was used to detect the expression of INPP5E in control, mimic-NC, and mimic-1 groups. (c) WB assay was used to detect the expression of INPP5E in control, mimic-NC, and mimic-1 groups. (d) The dual luciferase reporting assay was used to verify the binding of INPP5E to hsa-miR-181a-5p. (e) RT-PCR assay was used to detect the expression of hsa-miR-138-5p in control, mimic-NC, and mimic-2 groups. (f) RT-PCR assay was used to detect the expression of INPP5E in control, mimic-NC, and mimic-2 groups. (g) WB assay was used to detect the expression of INPP5E in control, mimic-NC, and mimic-2 groups. (h) The dual luciferase reporting assay was used to verify the binding of INPP5E to hsa-miR-138-5p. (i) StarBase database was used to predict the lncRNAs that might bind to hsa-miR-181a-5p and hsa-miR-138-5p. (j) RT-PCR assay was used to detect the expression of SNHG12 in control, NC, si-SNHG12-1, si-SNHG12-2, and si-SNHG12-3 groups. (k) RT-PCR assay was used to detect the expression of hsa-miR-181a-5p and hsa-miR-138-5p in control, NC, and si-SNHG12-3 groups. (l, m) The dual luciferase reporting assay was used to verify the binding of SNHG12 to hsa-miR-181a-5p and hsa-miR-138-5p. Notes: $^{*}p < 0.05$, $^{**}p < 0.01$, and $^{***}p < 0.001$ compared with the control.

(a)
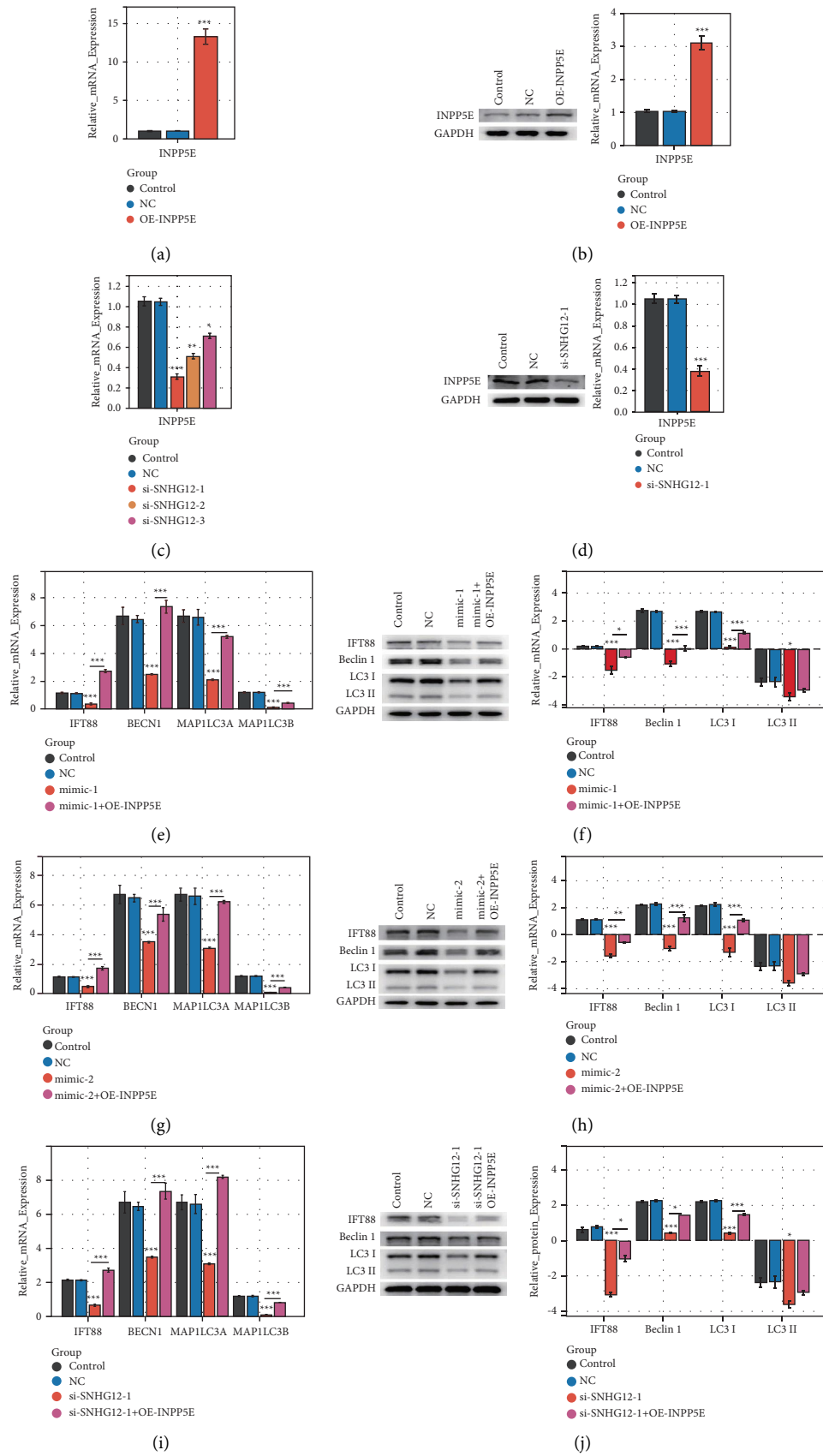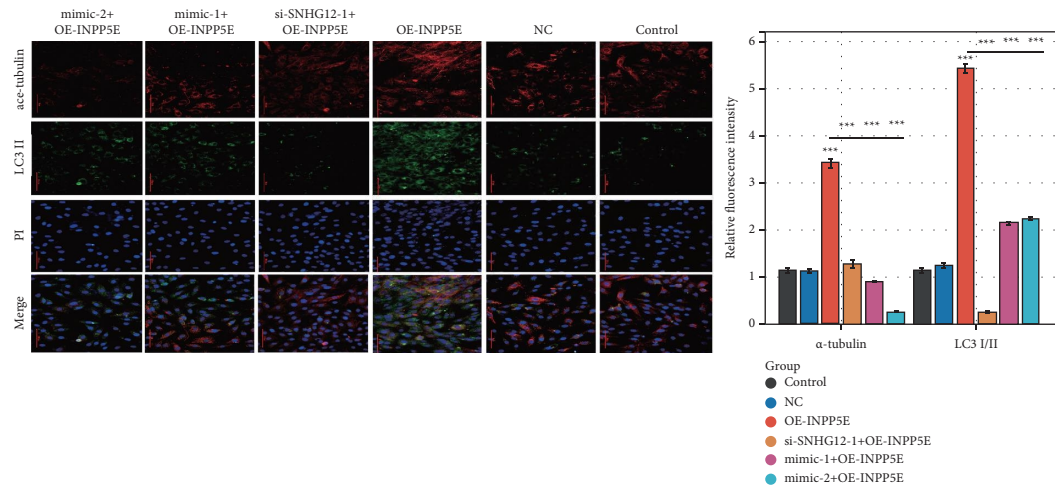
(b)

(c)

(d)

(e)

(f)

(g)

(h)

(i)

(j)

Figure 4: Continued.

(k)

FIGURE 4: Silencing SNHG12 promotes primary cilia and autophagy via the hsa-miR-181a-5p/hsa-miR-138-5p-INPP5E axis in vitro. (a, b) RT-PCR and WB assay were used to detect the expression of INPP5E in control, NC, and OE-INPP5E groups. (c, d) RT-PCR and WB assay were used to detect the expression of INPP5E in control, NC, and si-SNHG12 groups. (e, f) RT-PCR assay was used to detect the mRNA expression of IFT88, Beclin1, MAP1LC3A, and MAP1LC3B, and WB assay was used to detect the protein expression of IFT88, Beclin1, LC3 I, and LC3 II in control, NC, mimic-1, and mimic-1 + OE-INPP5E groups. (g, h) RT-PCR assay was used to detect the mRNA expression of IFT88, Beclin1, MAP1LC3A, and MAP1LC3B, and WB assay was used to detect the protein expression of IFT88, Beclin1, LC3 I, and LC3 II in control, NC, mimic-2, and mimic-2 + OE-INPP5E groups. (i, j) RT-PCR assay was used to detect the mRNA expression of IFT88, Beclin1, MAP1LC3A, and MAP1LC3B, and WB assay was used to detect the protein expression of IFT88, Beclin1, LC3 I, and LC3 II in control, NC, si-SNHG12-1, and si-SNHG12-1 + OE-INPP5E groups. (k) Ace-tubulin was used to label primary cilia, and LC3 II was used to label autophagy via immunofluorescence assay. Notes: $^* p < 0.05$, $^{**} p < 0.01$, and $^{***} p < 0.001$ compared with the control or between the indicated groups.

the protein expression of collagen II and cyclin D1 was reduced in the si-SNHG12 group (Figures 6(g) and 6(h)). Compared with the si-SNHG12 group, the mRNA expression of COL2A1 and CCND1 was increased and the protein expression of collagen II and cyclin D1 was increased in the si-SNHG12 + OE-INPP5E group (Figures 6(c) and 6(d)). Together, silencing SNHG12 inhibits the expression of collagen II and cyclin D1 via the hsa-miR-181a-5p/hsa-miR-138-5p-INPP5E axis in chondrocytes.

4. Discussion

Primary cilia are horn-like sensory organelles that play a crucial role in regulating the function of chondrocytes [21]. INPP5E regulates mitosis and is responsible for the ciliary disassembly of primary cilia [5]. However, the impact of INPP5E on primary cilia in chondrocytes has not yet been reported. IFT88 is a core component of the intraflagellar transport complex B and is essential for the construction of cilia [22]. Downregulation or loss of IFT88 is known to impair cilia occurrence [23]. Ace-tubulin, a notable protein, regulates ciliary peristalsis and controls its stability [24]. Our study found that silencing INPP5E inhibited the expression of both IFT88 and ace-tubulin, thereby indicating that the inhibition of INPP5E reduces primary cilia formation in chondrocytes.

Recent studies have demonstrated that the activation of autophagy requires primary cilia, and it is involved in controlling cilia formation [25]. In this study, chondrocytes were treated with CH, resulting in a significant reduction in

the expression of Beclin-1, LC3 I, and LC3 II. It has been positively associated that increased levels of Beclin-1, LC3 I, or LC3 II lead to autophagy [26, 27]. These findings further support the hypothesis that inhibition of primary cilia reduces the autophagy of chondrocytes. miRNAs, which are small noncoding RNAs, inhibit gene mRNA expression by interfering with transcription [28]. In this study, two miRNAs, hsa-miR-181a-5p and hsa-miR-138-5p, were found to bind with INPP5E and inhibit its expression. hsa-miR-181a-5p inhibits autophagy in MCF-10A cells [29], while hsa-miR-138-5p inhibits autophagy in pancreatic cancer cells [30]. Overexpression of hsa-miR-181a-5p or hsa-miR-138-5p inhibits Beclin-1, LC3 I, or LC3 II in chondrocytes. Moreover, it also inhibits the promoting effect of INPP5E on Beclin-1, LC3 I, or LC3 II in chondrocytes. Therefore, hsa-miR-181a-5p or hsa-miR-138-5p inhibits the autophagy of chondrocytes by inhibiting INPP5E.

The impact of hsa-miR-181a-5p or hsa-miR-138-5p on primary cilia has yet to be documented. In this current study, the overexpression of hsa-miR-181a-5p or hsa-miR-138-5p was found to inhibit IFT88 and ace-tubulin in chondrocytes, implying that autophagy of chondrocytes is inhibited by these miRNAs through the inhibition of primary cilia. Furthermore, overexpression of hsa-miR-181a-5p or hsa-miR-138-5p was found to counteract the promoting effect of INPP5E on IFT88 and ace-tubulin in chondrocytes. Therefore, the downregulation of chondrocyte autophagy can be attributed to the inhibition of inPP5E-induced primary cilia by hsa-miR-181a-5p or hsa-miR-138-5p.
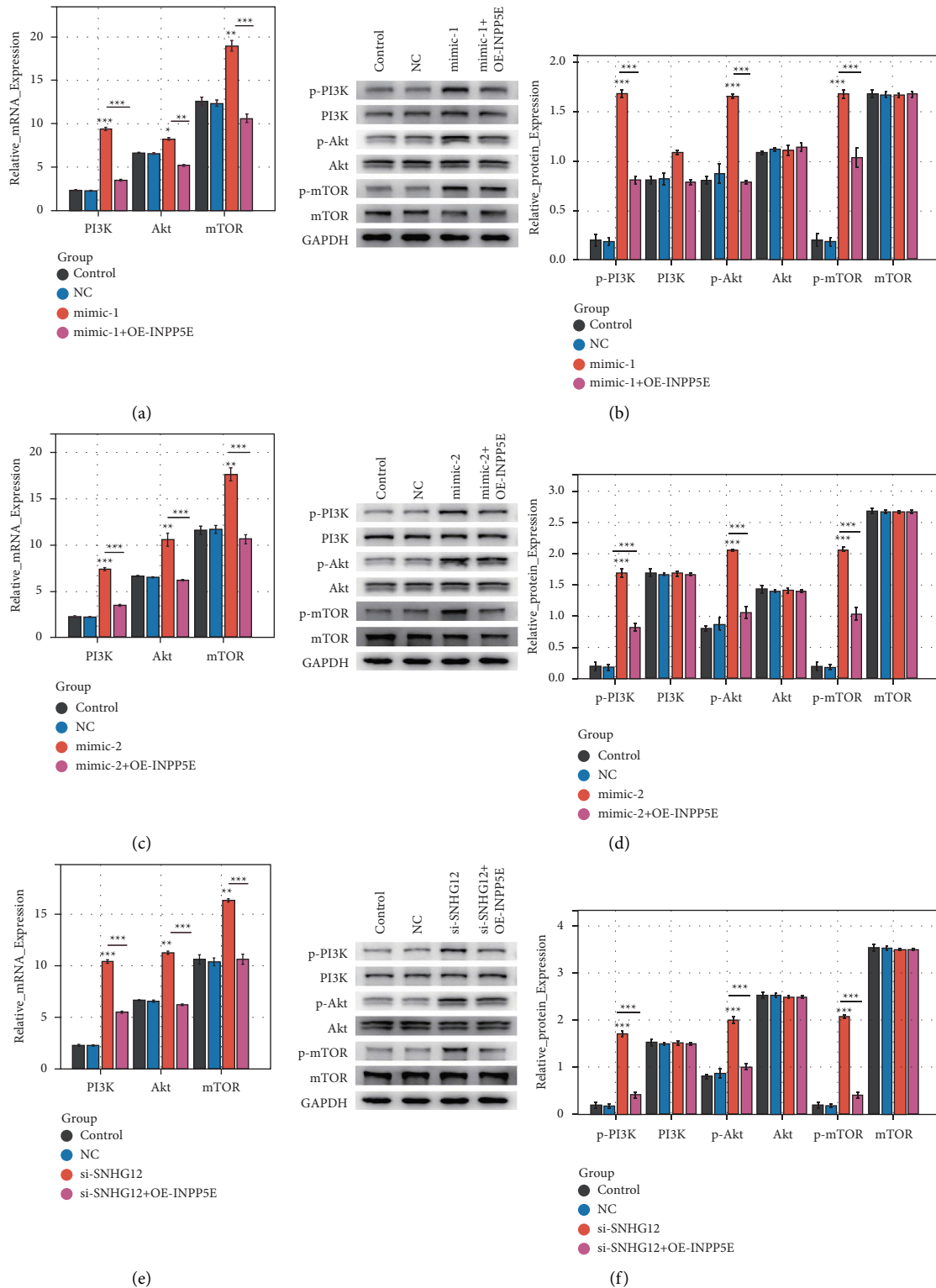
Figure 5: Silencing SNHG12 activated the PI3K-Akt-mTOR signaling pathway via the hsa-miR-181a-5p/hsa-miR-138-5p-INPP5E axis in vitro. (a) RT-PCR assay was used to detect the expression of PI3K, Akt, and mTOR in control, NC, mimic-1, and mimic-1 + OE-INPP5E groups. (b) WB assay was used to detect the expression of PI3K, p-PI3K, Akt, p-Akt, mTOR, and p-mTOR in control, NC, mimic-1, and mimic-1 + OE-INPP5E groups. (c) RT-PCR assay was used to detect the expression of PI3K, Akt, and mTOR in control, NC, mimic-2, and mimic-2 + OE-INPP5E groups. (d) WB assay was used to detect the expression of PI3K, p-PI3K, Akt, p-Akt, mTOR, and p-mTOR in control, NC, mimic-2, and mimic-2 + OE-INPP5E groups. (e) RT-PCR assay was used to detect the expression of PI3K, Akt, and mTOR in control, NC, si-SNHG12, and si-SNHG12 + OE-INPP5E groups. (f) WB assay was used to detect the expression of PI3K, p-PI3K, Akt, p-Akt, mTOR, and p-mTOR in control, NC, si-SNHG12, and si-SNHG12 + OE-INPP5E groups. Notes: $^{*}p < 0.05$, $^{**}p < 0.01$, and $^{***}p < 0.001$ compared with the control or between the indicated groups.
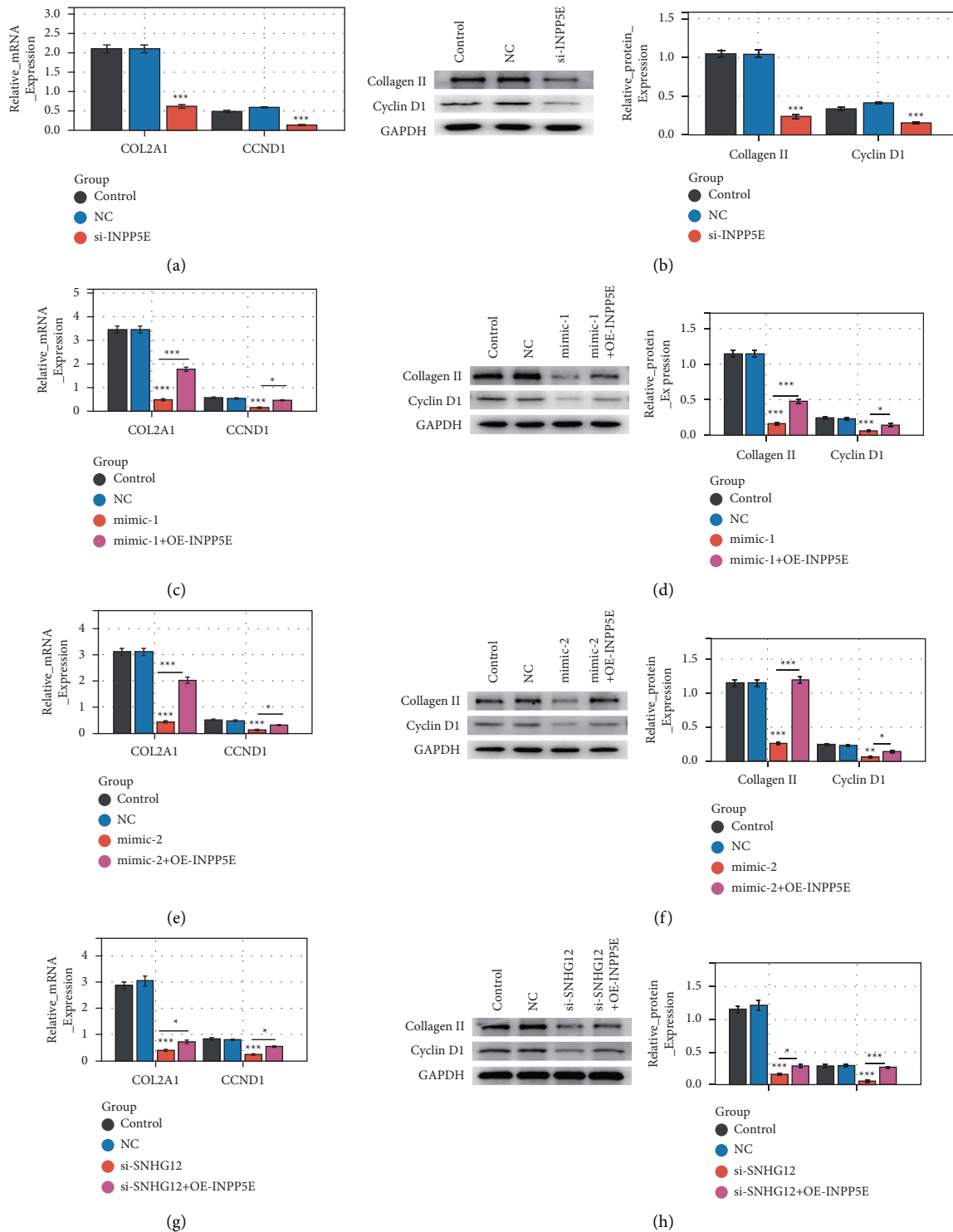
(a)

(b)

(c)

(d)

(e)

(f)

(g)

(h)

FIGURE 6: Silencing SNHG12 inhibits the expression of collagen II and cyclin D1 via the hsa-miR-181a-5p/hsa-miR-138-5p-INPP5E axis in vitro. (a) RT-PCR assay was used to detect the expression of COL2A1 and CCND1 in control, NC, and si-INPP5E groups. (b) WB assay was used to detect the expression of collagen II and cyclin D1 in control, NC, and si-INPP5E groups. (c) RT-PCR assay was used to detect the expression of COL2A1 and CCND1 in control, NC, mimic-1, and mimic-1 + OE-INPP5E groups. (d) WB assay was used to detect the expression of collagen II and cyclin D1 in control, NC, mimic-1, and mimic-1 + OE-INPP5E groups. (e) RT-PCR assay was used to detect the expression of COL2A1 and CCND1 in control, NC, mimic-2, and mimic-2 + OE-INPP5E groups. (f) WB assay was used to detect the expression of collagen II and cyclin D1 in control, NC, mimic-2, and mimic-2 + OE-INPP5E groups. (g) RT-PCR assay was used to detect the expression of COL2A1 and CCND1 in control, NC, si-SNHG12, and si-SNHG12 + OE-INPP5E groups. (h) WB assay was used to detect the expression of collagen II and cyclin D1 in control, NC, si-SNHG12, and si-SNHG12 + OE-INPP5E groups. $^{*}p < 0.05$, $^{**}p < 0.01$, and $^{***}p < 0.001$ compared with the control or between the indicated groups.

CeRNAs regulate the transcripts of shared miRNAs in a mutually inhibiting manner at the posttranscriptional level. This regulation creates a network between mRNAs and noncoding RNAs such as miRNAs, lncRNAs, and circRNAs. In this study, it was discovered that SNHG12 binds with hsa-miR-181a-5p or hsa-miR-138-5p, inhibiting their expression. SNHG12 has been reported to promote autophagy in previous studies, and this study confirmed its role in chondrocytes. Furthermore, silencing SNHG12 inhibits the promoting effect of INPP5E on Beclin-1, LC3 I, or LC3 II in chondrocytes. Thus, SNHG12 promotes chondrocyte autophagy through the hsa-miR-181a-5p/hsa-miR-138-5p-INPP5E axis. In addition, this study found that SNHG12 promotes the expression of IFT88 and ace-tubulin in chondrocytes, a finding not previously reported. Silencing SNHG12 also inhibits the promoting effect of INPP5E on IFT88 and ace-tubulin in chondrocytes. Therefore, SNHG12 promotes chondrocyte autophagy by promoting INPP5E-induced primary cilia formation.

The inhibition of mTORC1 signaling by primary cilia has been demonstrated in previous studies [6]. In our study, we observed an increase in protein expression of p-mTOR after treating chondrocytes with CH. Interestingly, treating chondrocytes with Rapa also led to elevated expression of ace-tubulin. This suggests the presence of an mTOR-primary cilia-mTOR loop in chondrocytes. mTOR is a highly conserved kinase that plays a crucial role in regulating autophagy [31]. In this study, we discovered that inhibiting mTOR promotes autophagy in chondrocytes. Furthermore, inhibiting INPP5E reduced the enhancing effect of Rapa on autophagy. Therefore, INPP5E promotes chondrocyte autophagy by inhibiting the mTOR-primary cilia-mTOR loop.

Collagen II is a cross-linked copolymer that forms the core fiber network during chondrogenesis [32]. The function of articular cartilage relies on the longevity of collagen II [33]. Silencing INPP5E inhibits the expression of collagen II in chondrocytes, while silencing SNHG12 or overexpression of hsa-miR-181a-5p or hsa-miR-138-5p inhibits the promoting effect of INPP5E on collagen II in chondrocytes. These findings suggest that SNHG12 promotes collagen II through the hsa-miR-181a-5p/hsa-miR-138-5p/INPP5E axis in chondrocytes. Chondrocytes require attachment to a matrix rich in collagen II for their proliferation and maturation [34], and therefore, SNHG12 might play a role in these processes. Dicam stimulates chondrocyte proliferation and maturation via the hedgehog signaling pathway in primary cilia [35]. Inhibition of the PI3K/AKT/mTOR signaling pathway impedes chondrocyte proliferation [36]. Therefore, SNHG12 may promote chondrocyte proliferation and maturation by activating the mTOR signal via INPP5E-mediated primary cilia formation.

Cyclin D1 integrates extracellular mitotic signaling with cell cycle progression [37]. Silencing INPP5E inhibits the expression of cyclin D1 in chondrocytes. In addition, silencing SNHG12 or overexpressing hsa-miR-181a-5p or hsa-miR-138-5p inhibits the promoting effect of INPP5E on cyclin D1 in chondrocytes. These results suggest that SNHG12 promotes collagen II via the hsa-miR-181a-5p/hsa-miR-138-5p- INPP5E axis in chondrocytes and might also maintain their cell cycle.

In conclusion, our study suggests that SNHG12 upregulates INPP5E by inhibiting hsa-miR-181a-5p/hsa-miR-138-5p in chondrocytes. This, in turn, increases autophagy in chondrocytes by deactivating the mTOR-primary cilia-mTOR loop. These findings provide a promising foundation for the development of targeted treatments for patients with cartilage-related diseases.

Data Availability

The datasets during and/or analyzed during the current study are available from the corresponding author on reasonable request.

Disclosure

A preprint has previously been published [38].

Conflicts of Interest

The authors declare that they have no conflicts of interest.

Authors' Contributions

All the authors participated in performing the experiments and writing the paper. Zhenkai Wu and Jing Ding supervised the study and revised the paper. Weijia Feng and Lei Liu contributed equally and share first authorship.

Acknowledgments

Supplementary Materials

Supplementary figure 1: the miRNAs that might bind to INPP5E predicted by the TargetScan database. Supplement table 1: the corresponding plasmids or siRNAs used in this study. Supplement table 2: all primers used in this study. Supplement table 3: the antibodies used in this study. Supplement material (not for publication): original protein expression bands. (*Supplementary Materials*)

References

[1] Y. Krishnan and A. J. Grodzinsky, "Cartilage diseases," *Matrix Biology*, vol. 71-72, pp. 51–69, 2018.

[2] A. C. Hall, "The role of chondrocyte morphology and volume in controlling phenotype-implications for osteoarthritis, cartilage repair, and cartilage engineering," *Current Rheumatology Reports*, vol. 21, no. 8, p. 38, 2019.

[3] F. Tao, T. Jiang, H. Tao, H. Cao, and W. Xiang, "Primary cilia: versatile regulator in cartilage development," *Cell Proliferation*, vol. 53, no. 3, Article ID e12765, 2020.

[4] R. Zhang, J. Tang, T. Li, J. Zhou, and W. Pan, "INPP5E and coordination of signaling networks in cilia," *Frontiers in Molecular Biosciences*, vol. 9, Article ID 885592, 2022.

[5] O. V. Plotnikova, S. Seo, D. L. Cottle et al., "INPP5E interacts with AURKA, linking phosphoinositide signaling to primary cilium stability," *Journal of Cell Science*, vol. 128, no. 2, pp. 364–372, 2015.

[6] Y. Lai and Y. Jiang, "Reciprocal regulation between primary cilia and mTORC1," *Genes*, vol. 11, no. 6, p. 711, 2020.

[7] J. Y. Ko, E. J. Lee, and J. H. Park, "Interplay between primary cilia and autophagy and its controversial roles in cancer," *Biomolecules and Therapeutics*, vol. 27, no. 4, pp. 337–341, 2019.

[8] R. Duan, H. Xie, and Z. Z. Liu, "The role of autophagy in osteoarthritis," *Frontiers in Cell and Developmental Biology*, vol. 8, Article ID 608388, 2020.

[9] T. Noda, "Regulation of autophagy through TORC1 and mTORC1," *Biomolecules*, vol. 7, no. 4, p. 52, 2017.

[10] D. W. Thomson and M. E. Dinger, "Endogenous microRNA sponges: evidence and controversy," *Nature Reviews Genetics*, vol. 17, no. 5, pp. 272–283, 2016.

[11] J. Hao, H. Mei, Q. Luo et al., "TCL1A acts as a tumour suppressor by modulating gastric cancer autophagy via miR-181a-5p-TCL1A-Akt/mTOR-c-MYC loop," *Carcinogenesis*, vol. 44, no. 1, pp. 29–37, 2023.

[12] B. A. Kang, H. M. Li, Y. T. Chen et al., "High-density lipoprotein regulates angiogenesis by affecting autophagy via miRNA-181a-5p," *Science China Life Sciences*, vol. 67, no. 2, pp. 286–300, 2023.

[13] F. Liu, Y. Yang, W. Peng et al., "Mitophagy-promoting miR-138-5p promoter demethylation inhibits pyroptosis in sepsis-associated acute lung injury," *Inflammation Research*, vol. 72, no. 2, pp. 329–346, 2023.

[14] J. Ma, Y. Zhang, H. Ji et al., "Overexpression of miR-138-5p suppresses MnCl2-induced autophagy by targeting SIRT1 in SH-SY5Y cells," *Environmental Toxicology*, vol. 34, no. 4, pp. 539–547, 2019.

[15] Y. Yan, L. Chen, J. Zhou, and L. Xie, "SNHG12 inhibits oxygen-glucose deprivation-induced neuronal apoptosis via the miR-181a-5p/NEGR1 axis," *Molecular Medicine Reports*, vol. 22, no. 5, pp. 3886–3894, 2020.

[16] L. Yan, L. Li, and J. Lei, "Long noncoding RNA small nucleolar RNA host gene 12/microRNA-138-5p/nuclear factor I/B regulates neuronal apoptosis, inflammatory response, and oxidative stress in Parkinson's disease," *Bioengineered*, vol. 12, no. 2, pp. 12867–12879, 2021.

[17] Y. H. Li, D. Zhu, Z. Cao, Y. Liu, J. Sun, and L. Tan, "Primary cilia respond to intermittent low-magnitude, high-frequency vibration and mediate vibration-induced effects in osteoblasts," *American Journal of Physiology-Cell Physiology*, vol. 318, no. 1, pp. C73–C82, 2020.

[18] W. Sun, Y. Li, and S. Wei, "miR-4262 regulates chondrocyte viability, apoptosis, autophagy by targeting SIRT1 and activating PI3K/AKT/mTOR signaling pathway in rats with osteoarthritis," *Experimental and Therapeutic Medicine*, vol. 15, no. 1, pp. 1119–1128, 2018.

[19] L. Chang, X. Chai, P. Chen, J. Cao, H. Xie, and J. Zhu, "miR-181b-5p suppresses starvation-induced cardiomyocyte autophagy by targeting Hspa5," *International Journal of Molecular Medicine*, vol. 43, no. 1, pp. 143–154, 2019.

[20] X. Yao, R. Yao, F. Huang, and J. Yi, "LncRNA SNHG12 as a potent autophagy inducer exerts neuroprotective effects against cerebral ischemia/reperfusion injury," *Biochemical and Biophysical Research Communications*, vol. 514, no. 2, pp. 490–496, 2019.

[21] E. R. Moore and C. R. Jacobs, "The primary cilium as a signaling nexus for growth plate function and subsequent skeletal development," *Journal of Orthopaedic Research*, vol. 36, no. 2, pp. 533–545, 2018.

[22] C. Boehlke, H. Janusch, C. Hamann et al., "A cilia independent role of ift88/polaris during cell migration," *PLoS One*, vol. 10, Article ID e0140378, 2015.

[23] J. A. Follit, F. Xu, B. T. Keady, and G. J. Pazour, "Characterization of mouse IFT complex B," *Cell Motility and the Cytoskeleton*, vol. 66, no. 8, pp. 457–468, 2009.

[24] D. Wloga, E. Joachimiak, P. Louka, and J. Gaertig, "Post-translational modifications of tubulin and cilia," *Cold Spring Harbor Perspectives in Biology*, vol. 9, no. 6, Article ID a028159, 2017.

[25] O. Pampliega and A. M. Cuervo, "Autophagy and primary cilia: dual interplay," *Current Opinion in Cell Biology*, vol. 39, pp. 1–7, 2016.

[26] Y. J. Hu, J. T. Zhong, L. Gong, S. C. Zhang, and S. H. Zhou, "Autophagy-related beclin 1 and head and neck cancers," *OncoTargets and Therapy*, vol. 13, pp. 6213–6227, 2020.

[27] B. L. Heckmann and D. R. Green, "LC3-associated phagocytosis at a glance," *Journal of Cell Science*, vol. 132, no. 5, Article ID jcs222984, 2019.

[28] L. Chen, L. Heikkinen, C. Wang, Y. Yang, H. Sun, and G. Wong, "Trends in the development of miRNA bioinformatics tools," *Briefings in Bioinformatics*, vol. 20, no. 5, pp. 1836–1852, 2019.

[29] J. L. Wei, Y. C. Li, Z. L. Ma, and Y. X. Jin, "MiR-181a-5p promotes anoikis by suppressing autophagy during detachment induction in the mammary epithelial cell line MCF10A," *Protein Cell*, vol. 7, no. 4, pp. 305–309, 2016.

[30] S. Tian, X. Guo, C. Yu, C. Sun, and J. Jiang, "miR-138-5p suppresses autophagy in pancreatic cancer by targeting SIRT1," *Oncotarget*, vol. 8, no. 7, pp. 11071–11082, 2017.

[31] Y. Wang and H. Zhang, "Regulation of autophagy by mTOR signaling pathway," *Advances in Experimental Medicine and Biology*, vol. 1206, pp. 67–83, 2019.

[32] D. Eyre, "Collagen of articular cartilage," *Arthritis Research*, vol. 4, no. 1, pp. 30–35, 2002.

[33] M. L. Tiku and B. Madhan, "Preserving the longevity of long-lived type II collagen and its implication for cartilage therapeutics," *Ageing Research Reviews*, vol. 28, pp. 62–71, 2016.

[34] L. Terpstra, J. Prud'homme, A. Arabian et al., "Reduced chondrocyte proliferation and chondrodysplasia in mice lacking the integrin-linked kinase in chondrocytes," *The Journal of Cell Biology*, vol. 162, no. 1, pp. 139–148, 2003.

[35] S. Han, H. R. Park, E. J. Lee et al., "Dicam promotes proliferation and maturation of chondrocyte through Indian hedgehog signaling in primary cilia," *Osteoarthritis and Cartilage*, vol. 26, no. 7, pp. 945–953, 2018.

[36] F. B. Feng and H. Y. Qiu, "RETRACTED: effects of Artesunate on chondrocyte proliferation, apoptosis and autophagy through the PI3K/AKT/mTOR signaling pathway in rat models with rheumatoid arthritis," *Biomedicine and Pharmacotherapy*, vol. 102, pp. 1209–1220, 2018.

[37] G. Tchakarska and B. Sola, "The double dealing of cyclin D1," *Cell Cycle*, vol. 19, no. 2, pp. 163–178, 2020.

[38] J. Ding, S. Lin, L. Liu, Z. Wu, and W. Feng, "SNHG12 promotes chondrocyte autophagy by blocking he mTOR-primary cilia-mTOR loop via activating the miR-181a-5p/miR-138-5p-INPP5E axis," 2022, https://www.researchsquare.com/article/rs-1622727/v1.